Study of the Electronic Structure of Ni(η^5-C_5H_5)(NO) by Variable-Photon-Energy Photoelectron Spectroscopy and Density Functional Calculations

Christian N. Field,[†] Jennifer C. Green,*[,†] Markus Mayer,[‡] Vladimir A. Nasluzov,[‡,§] Notker Rösch,*[,‡] and Michele R. F. Siggel[||]

Inorganic Chemistry Laboratory, University of Oxford, South Parks Road, Oxford OX1 3QR, U.K., Lehrstuhl für Theoretische Chemie, Technische Universität München, D-85747 Garching, Germany, and EPSRC Daresbury Laboratory, Daresbury, Warrington WA4 4AD, U.K.

Received August 24, 1995[⊗]

Photoelectron spectra, with photon energies varying from 18 to 120 eV, have been measured for Ni(η^5-C_5H_5)(NO). Relative partial photoelectron cross sections and branching ratios have been evaluated for the first three valence ionization bands. He I and He II photoelectron spectra have been remeasured for Ni(η^5-C_5H_5)(NO) and Ni(η^5-$C_5H_4CH_3$)(NO). In the latter case, the fine structure on the first band differs from that in the previously published spectrum. Density functional calculations have been carried out to determine the ionization potentials of the lowest lying states of Ni(η^5-C_5H_5)(NO) as well as the corresponding photoionization cross sections and the resulting branching ratios using the LCGTO-DF and LDKL-DF methods, respectively. Both experimental and theoretical investigations lead to an ion state ordering $^2E_1 < {}^2E_2 \sim {}^2A_1 < {}^2E_1$ and an assignment of $^2E_1$ states to the first and third bands with the $^2A_1$ and $^2E_2$ states comprising the second band. This differs from the original assignment in the literature, where the $^2A_1$ ionization was assigned to a high-energy shoulder on the first band. The separation of this shoulder from the main band maximum of 0.23 eV (1850 ± 81 cm^{-1}) suggests that it may be caused by excitation of the NO stretching vibration in the ion. The neutral molecule has a NO stretch of 1832 cm^{-1}; the calculated energies for the neutral molecule and the cation are 1845 and 1911 cm^{-1}, respectively. Agreement between calculated and experimental ionization energies and good matching of the theoretical and measured branching ratios support the new assignment of the photoelectron spectrum.

Introduction

The high symmetry and volatility of (η^5-cyclopentadienyl)-nitrosylnickel, Ni(η^5-C_5H_5)(NO), made it an early candidate for investigation by photoelectron (PE) spectroscopy.[1] Four primary ionization processes were deemed to fall in the ionization energy (IE) region below 12 eV associated with $^2A_1$, $^2E_2$, and two $^2E_1$ ion states, though only three well-resolved bands are observed. An assignment of the first band to a combination of $^2E_1$ and $^2A_1$ ion states was made on the basis of a high-energy shoulder observed on this band and as a result of *ab initio* SCF−MO calculations.[1,2] The second band was assigned to the $^2E_2$ ion state and the third to the higher lying $^2E_1$ ion state. Subsequent calculations have not challenged this assignment[3−5] though none have managed to reproduce the observed pattern of ionzation bands very well. Also the variation of the proportion of Ni, cyclopentadienyl, and nitrosyl character in the molecular orbitals (MOs) $7e_1$ and $8e_1$ varies considerably according to the calculation method (see Table 1).

Nickel presents a particular challenge in the prediction of ionization energies of its compounds as the d electrons experience considerable stabilization on ionization. Variable-photon-energy PE spectroscopy has proved a valuable technique for unambiguous assignment of PE bands, establishing the covalent nature of particular molecular orbitals and, in favorable circumstances, being able to give quantitative estimates of the relative metal and ligand characters for the corresponding orbitals.[6] We therefore decided to obtain cross section and branching ratio data over a wide range of photon energies on the low-energy PE bands of Ni(η^5-C_5H_5)(NO) in order to obtain further insight into the electronic structure of this prototypical molecule. In the course of this study, doubt was cast on the validity of the literature PE spectrum of Ni(η^5-$C_5H_4CH_3$)(NO),[1] so this was remeasured.

The experimental study was supported by electronic structure calculations using the linear combination of Gaussian-type orbital density functional (LCGTO-DF) method.[7] Various ground state properties were determined as well as the lower

Table 1. Compositions[a] of the Four Highest Occupied and the Lowest Unoccupied Orbitals ($9e_1$) of Ni(η^5-C_5H_5)(NO) According to Various Methods of Calculation in Terms of Percent Ni/Cyclopentadienyl/Nitrosyl

MO	HF−SCF[b]	INDO[c]	MS−Xα[d]	LCGTO-DF[e]
$9e_1$			18/6/34	26(25)/13/61
$8e_1$	18/63/19	9/79/12	28/32/10	22(15)/49/29
$15a_1$	72/12/8	90/3/7	84/1/2	91(77)/3/6
$4e_2$	74/23/0	97/3/0	94/1/0	96(96)/4/0
$7e_1$	60/28/10	45/49/6	59/23/3	51(50)/42/7

[a] Based on Mulliken populations except for the MS−Xα results, where the localization within the various atomic spheres is given; the intersphere and the outer-sphere contributions are omitted. [b] References 1 and 2. [c] References 3 and 4. [d] Reference 5. [e] Present work; Mulliken populations from the LDA calculation at the GGA-optimized geometry. For Ni, the d contribution is given in parentheses.

[†] University of Oxford.
[‡] Technische Universität München.
[§] Permanent address: Institute of Chemistry of Natural Organic Materials, Russian Academy of Science, 660049 Krasnoyarsk, Russia.
[||] EPSRC Daresbury Laboratory.
[⊗] Abstract published in *Advance ACS Abstracts,* April 1, 1996.

(1) Evans, S.; Guest, M. F.; Hillier, I. H.; Orchard, A. F. *J. Chem. Soc., Faraday Trans. 2* **1974**, 417−421.
(2) Hillier, I. H.; Saunders, V. R. *Mol. Phys.* **1972**, *23*, 449−456.
(3) Böhm, M. C. *Z. Naturforsch.* **1981**, *36A*, 1361−1366.
(4) Böhm, M. C. *J. Chem. Phys.* **1983**, *12*, 7044−7064.
(5) Modelli, A.; Foffani, A.; Scagnolari, F.; Torroni, S.; Guerra, M.; Jones, D. *J. Am. Chem. Soc.* **1989**, *111*, 6040−6045.
(6) Green, J. C. *Acc. Chem. Res.* **1994**, *27*, 131−137.
(7) Dunlap, B. I.; Rösch, N. *Adv. Quantum Chem.* **1990**, *21*, 317.

0020-1669/96/1335-2504$12.00/0

lying ionization energies. Furthermore, cross sections and branching ratios were calculated for the photoionization processes involving the four cation states in question. For this purpose, the recently developed logarithmic derivative Kohn−Lobatto density functional (LDKL-DF) method was employed.[8,9] This computational approach to electronic continuum wave functions employs the full molecular electronic potential as obtained by the LCGTO-DF method. The LDKL-DF method has proven to be a useful and reliable tool for calculating photoionization cross sections of both valence and core level processes of a variety of molecules.[9−11] It is important to note that in the present calculations both initial and final states of the photoelectron process are described without invoking the muffin-tin approximation to the molecular electronic potential. This approximation is instrumental for applying the multiple-scattering technique that forms the basis of many photoionsation cross section calculations on larger molecules.[12−15] However, it is well-known that the muffin-tin approximation is particularly severe and unreliable for molecules exhibiting an open structure like Ni(η^5-C_5H_5)(NO) (**1**).[16]

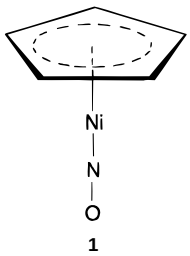

1

Experimental and Computational Details

Preparation of Ni(η^5-C_5H_5)(NO) and Ni(η^5-$C_5H_4CH_3$)(NO). Ni(η^5-C_5H_5)(NO) (**1**) was synthesized according to the method used by King.[17] Ni(η^5-$C_5H_4CH_3$)(NO) was synthesized in a similar way with the modification that Na($C_5H_4CH_3$) was used in place of cyclopentadiene. Both compounds were isolated by sublimation, using a Pardy apparatus.[18] Purity was confirmed by ^{1}H NMR of Ni(η^5-C_5H_5)(NO) in C_6D_6, $\delta = 4.98$ ppm (singlet), and Ni(η^5-$C_5H_4CH_3$)(NO) in $CDCl_3$, $\delta = 2.39$ (singlet), 5.24 (doublet), 5.26 (doublet) ppm.

Variable-Photon-Energy PE Spectroscopy. Synchrotron radiation from the 2 GeV electron storage ring at the Daresbury Laboratory was monochromated for this experiment using a toroidal grating monochromator (TGM) on beamline 3.3. The TGM was used with fixed entrance and exit slit widths of 5.5 mm. Two gratings were employed covering the photon energy ranges 10−50 eV (710 lines/mm) and 50−120 eV (2400 lines/mm). The photons were introduced to the ionization region via a glass light guide, 2 mm in diameter. Due to the partial polarization of the incident synchrotron radiation, the lens and analyzer were positioned at the "magic angle" with respect to the plane of polarization of the light so that the photoionization cross sections and thus intensities of the various ionization bands were not affected by the photoelectron asymmetry parameter, β.

The experiment was carried out using the chemical angle resolved photoelectron spectrometer, CARPES, which will be described elsewhere.[19] The sample of Ni(η^5-C_5H_5)(NO) was introduced into the ionization region via a $^1/_8$ in. o.d. pipe, and the vapor pressure in the chamber was controlled by a needle valve in the sample line. The sample was degassed through several freeze−pump−thaw cycles. A liquid-nitrogen-cooled cold finger was used to prevent diffusion of the compounds into the rotary pump. The photoelectrons were energy-analysed using the focusing action of a three-element zoom lens to accelerate or retard the electrons, followed by a hemispherical analyzer of mean radius 45 mm which was operated at a pass energy of 4.603 eV for photon energies 18−40 eV and at a pass energy of 9.207 eV for photon energies above 40 eV. A position-sensitive multichannel detector was used consisting of a pair of chevroned multichannel plates backed by a resistive anode. The decay of the electron current in the storage ring was corrected by measuring the current in a fine tungsten mesh positioned in the path of the radiation at the exit of the ionization region. The performances of the tungsten mesh and the analyzer were estimated by measuring the intensity variation of several rare gases over the photon energy region of interest and comparing these with literature values for the cross sections.[20,21] Fluctuations in sample pressure were estimated by recording a calibration spectrum of the compound at a constant photon energy before and after every data spectrum. Variation in intensities between these calibration spectra was then interpreted as a measure of pressure fluctuation of the sample. The method of data analysis and estimated errors involved have been described elsewhere.[22,23] Bands A (A_1, A_2, and A_3), B, and C were fitted using asymmetric Gaussian functions.

He I and He II PE Spectroscopy. He I and He II spectra of Ni(η^5-C_5H_5)(NO) and Ni(η^5-$C_5H_4CH_3$)(NO) were obtained on a PES Laboratories 0078 spectrometer. The spectra were calibrated using He, Xe, and N_2. The spectrometer resolution was 27 meV (N_2 fwhm).

Density Functional Calculations, and Ground State Properties. The linear combination of Gaussian-type orbital density functional (LCGTO-DF) method[7] provides an efficient way for solving the effective one-electron equations resulting in the Kohn−Sham approach to density functional theory. A characteristic feature of this method is the use of three Gaussian-type basis sets, one for representing the molecular orbitals and two auxiliary basis sets to approximate the electronic charge density and the exchange-correlation potential, respectively. The exchange-correlation potential was used self-consistently in the local density approximation (LDA) without[24] and with density gradient corrections (generalized gradient approximation, GGA). GGA corrections were applied both to the exchange[25] and to the correlation functional.[26,27] A geometry optimization was carried out at both levels of theory, LDA and GGA, with the help of the variable-metric update scheme[28] using analytic energy derivatives[29,30] recently implemented in the LCGTO-DF program package.[31] The second derivatives of the total energy and thus the vibrational frequencies were calculated by finite differences of the energy gradients.

For the atoms C, N, and O, (9s,5p) orbital basis sets were used,[32] each augmented by a d-type polarization exponent[33] and contracted to [5p,4p,1d]. For H, a (6s) basis set,[32] augmented by a p-type polarization exponent,[33] was contracted to [4s,1p]. For Ni, the same orbital basis

(8) Rösch, N.; Wilhelmy, I. *Chem. Phys. Lett.* **1992**, *189*, 499.
(9) Wilhelmy, I.; Ackermann, L.; Görling, N.; Rösch, N. *J. Chem. Phys.* **1994**, *100*, 2808.
(10) Wilhelmy, I.; Rösch, N. *Chem. Phys.* **1994**, *185*, 317.
(11) Wilhelmy, I.; Laffon, C.; Ehrke, H.-U.; Wurth, W.; Rösch, N. *J. Phys. Chem.* **1995**, *99*, 8496.
(12) Dill, D.; Dehmer, J. L. *J. Chem. Phys.* **1974**, *61*, 692.
(13) Dehmer, J. L. In *Photophysics and Photochemistry in the Vacuum Ultraviolet*; McGlynn, S. P., Findley, G. L., Huebner, R. H., Eds.; NATO Advanced Study Institue, Series C, Vol. 142; Reidel: Dordrecht, The Netherlands, 1985; p 341.
(14) Stöhr, J. *NEXAFS Spectrocopy*; Springer: New York, 1992.
(15) Li, X.; Tse, J. S.; Bancroft, G. M.; Puddephatt, R. J.; Tan, K. H. *Inorg. Chem.*, **1996**, *35*, 2515.
(16) Schichl, A.; Menzel, D.; Rösch, N. *Chem. Phys. Lett.* **1984**, *105*, 285.
(17) King, R. B. *Organometallic Syntheses*; Academic Press: New York, 1965; Vol. 1, pp 169−171.
(18) Pardy, R. B. A. D.Phil. Thesis, Oxford University, 1977.
(19) Field, C. N.; Green, J. C.; Siggel, M. To be published.
(20) West, J. B.; Marr, G. V. *Proc. R. Soc. London A* **1976**, *349*, 397.
(21) West, J. B.; Morton, J. *At. Data Nucl. Data Tables* **1978**, *22*, 103.
(22) Cooper, G. C.; Green, J. C.; Dobson, B. R.; Hillier, I. H. *J. Am. Chem. Soc.* **1987**, *109*, 3836−3843.
(23) Cooper, G. C.; Green, J. C.; Payne, M. P. *Mol. Phys.* **1988**, *63*, 1031−1051.
(24) Vosko, S. H.; Wilk, L.; Nusair, M. *Can. J. Phys.* **1980**, *58*, 1200.
(25) Becke, A. D. *Phys. Rev. A* **1988**, *38*, 3098.
(26) Perdew, J. P. *Phys. Rev. B* **1986**, *33*, 8822.
(27) Perdew, J. P. *Phys. Rev. B* **1986**, *34*, 7046.
(28) Gill, P.; Murray, M.; Wright, M. H. *Practical Optimization*; Academic Press: London, 1981.
(29) Dunlap, B. I.; Andzelm, J.; Mintmire, J. W. *Phys. Rev. A* **1990**, *11*, 6354.
(30) Andzelm, J.; Wimmer, E. *J. Chem. Phys.* **1992**, *96*, 1280.
(31) Nasluzov, V.; Rösch, N. Unpublished.
(32) van Duijneveldt, F. B. *IBM Res. Rep.* **1971**, No. RJ 945.
(33) Huzinaga, S., Ed. *Gaussian Basis Sets for Molecular Calculations*; Elsevier: New York, 1984.

Table 2. Bond Distances d (Å) and Angles ∠ (deg) as Well as Harmonic Vibrational Frequencies ν (cm^{-1}) of Ni(η^5-C_5H_5)(NO) and the Cation Ni(η^5-C_5H_5)$(NO)^+$ As Obtained from LCGTO-DF Calculations at the LDA and GGA Levels of Theory Compared to Experiment[a]

	Ni(η^5-C_5H_5)(NO)			Ni(η^5-C_5H_5)$(NO)^+$	
	LDA	GGA	expt	LDA	GGA
d(Ni−C)	2.063	2.118	2.11[b]	2.063	2.120
d(Ni−N)	1.608	1.637	1.626[b]	1.666	1.697
d(N−O)	1.164	1.178	1.165[b]	1.120	1.152
d(C−C)	1.422	1.435	1.43[b]	1.426	1.440
d(C−H)	1.091	1.088	1.09[b]	1.093	1.089
∠N−Ni−C	144.1	144.8	144.8[b]	144.0	144.7
∠Ni−C−H	124.6	124.0	125.2[b]	124.4	124.1
ν(C−H str)	3162	3167	3110[c]	3154	3168
ν(C−C str)	1134	1106	1102[c]	1123	1095
ν(C−H bend)	772	777	820[c]	788	792
ν(Ni−N)	691	652		593	547
ν(Ni−Cp)	351	321		353	321
ν(N−O)	1928	1845	1832[d]	1989	1911
ν(N−O, free molecule)	1932	1865	1876[e]		
ν(N−O, free cation)			2344[e]	2408	2349

[a] Only totally symmetric vibrational modes with respect to C_{5v} symmetry have been calculated. For comparison, vibrational frequencies for the molecule NO and the cation NO^+ are also given. [b] Reference 36. [c] Values of ferrocene, Fe(η^5-C_5H_5)$_2$, for comparison.[38] [d] Reference 39. [e] Reference 40.

set, (15s,11p,6d) → [7s,6p,3d],[34] as in previous calculations was employed. The contraction of the orbital basis sets was based on atomic LDA eigenvectors. The exponents of the *s*- and r^2-type auxiliary fitting functions were obtained by appropriately scaling the s and p orbital exponents and by adding p- and d-type polarization functions.[7]

The molecular structure of Ni(η^5-C_5H_5)(NO) has been established from gas phase electron diffraction[35] and microwave[36] studies. The Ni−N−O link is linear, and this axis is coincident with the C_5 axis of rotation of the cyclopentadienyl ring (see **1**). Overall the molecule has C_{5v} symmetry which is imposed as a constraint in all calculations, and by convention the 5-fold axis is taken as the *z* direction.

In Table 2 the results of a geometry optimization, at both the LDA and the GGA level of theory, are compared to experiment. Both approximations for the exchange-correlation functional lead to rather similar geometries, in satisfactory agreement with experiment.[36] As is often found, all bond distances slightly elongate when density gradient corrections (GGA) are added to LDA, with the Ni−C and the Ni−N distances changing most significantly. However, the GGA value for d(Ni−C) agrees significantly better with experiment.[36] In any case, the present GGA results confirm an earlier DF calculation[37] carried out with a different computational procedure that also agreed much better with the structure of a microwave study[36] than with a more recent electron diffraction analysis.[35] We also were interested in the change of the geometry due to ionization of the HOMO $8e_1$. In Table 2 we display the optimized geometry for the cation Ni(η^5-C_5H_5)$(NO)^+$ in the state $^2E_1$. As in the case of the neutral molecule, the two approximations to the exchange-correlation functional, LDA and GGA, lead to similar geometries, differing significantly only in the Ni−C distance. The effect of ionization is also comparable in both methods: while the Ni−N distance is elongated by about 0.06 Å in either approximation, the N−O distance is shortened by 0.044 Å in LDA and 0.028 Å in GGA.

In the present investigation, only frequencies of vibrational modes which are totally symmetric with respect to C_{5v} symmetry were calculated (see Table 2). The results for the LDA and GGA calculations are in general very similar; for the modes assigned to deformations of the cyclopentadienyl ring, agreement with the experimental results of the corresponding modes of ferrocene, Fe(η^5-C_5H_5)$_2$, is very satisfactory.[38] A noteworthy difference between the LDA and the GGA results is observed for the N−O stretching mode where the GGA value agrees significantly better with experiment.[39] An analogous observation holds for the vibrational frequency calculated for the stretching frequency of the free NO molecule (see Table 2).[40] The experimentally determined difference of these two frequencies, $\Delta\nu$(NO) = ν(NO) − ν(NO free molecule) = −44 cm^{-1}, is much improved in GGA, −20 cm^{-1}, over the LDA value, −4 cm^{-1}. Back-donation from the fragment Ni(η^5-C_5H_5) lowers the diagonal N−O force constant in Ni(η^5-C_5H_5)(NO), corresponding to a frequency shift of about −100 cm^{-1}, but a rather strong coupling of the N−O stretch with the lower lying Ni−N stretching mode reduces this frequency lowering significantly. Apparently GGA provides a better description of this coupling and thus of this cancellation effect in the N−O frequency shift. The effect of ionization on the vibrational frequencies of the cation is of particular importance in the present work. As for the neutral molecule, both theoretical approaches, LDA and GGA, yield rather similar vibrational frequencies for the cation in its optimized geometry (Table 2), again with the exception of the vibrational modes affected by the NO ligand. Furthermore, the same modes with NO participation are the only ones that are significantly affected by ionization. Both methodological variants predict an increase of the N−O stretching frequency by about 70 cm^{-1} and a decrease of the N−Ni stretching frequency by 100 cm^{-1} upon going from the neutral to the cation. The excellent agreement of calculated and experimental vibrational frequencies for the free molecule NO and the free cation NO^+ (see Table 2) underlines the quality of the present computational approach.

Continuum Wave Function and Photoionization Calculations. Within the logarithmic derivative Kohn−Lobatto density functional (LDKL-DF) approach to photoionization,[8,9] cross sections are calculated in the dipole approximation after generation of one-electron final state continuum wave functions. The LDKL method employs a partitioning of space into a finite "reaction volume" and the complemetary asymptotic region where photoelectrons are subject only to a pure Coulomb attraction. Inside the reaction volume (in the present calculation a sphere of radius 35 au), the continuum wave function is determined via an algebraic variational principle after choosing a suitable basis set. To achieve the high flexibility required for a continuum wave function, a Gaussian-type basis set similar to the one used in the ground state calculations is augmented by so-called Lobatto shape functions, products of a polynomial in the radial part and a spherical harmonic. For valence shell photoionization processes considered in the present work, the one-electron potential obtained from a LCGTO-DF ground state LDA calculation provides an adequate description of the interaction of the photoelectron and the remaining ion.[9]

Since ionization connects atomic s-, p-, and d-type ground state orbitals to predominantly p-, d-, and f-type final state orbitals, respectively, GTO functions of the latter type are required for a proper description of the continuum. Accordingly, the Gaussian-type basis sets of C, N, and O described above were augmented by one diffuse s- and p-type exponent each, generated by continuing the last two GTO exponents of the corresponding type in the fashion of a geometrical series. Furthermore, a set of 5 d exponents was generated from two d-type polarization exponents[33] in the same spirit. The GTO ground state MO basis set for Ni was augmented by 9 f-type exponents to describe properly the metal-centered d → f ionization processes. In addition, Lobatto functions of order 60 were employed with angular components up to $l = 8$. For the evaluation of the corresponding matrix elements, the multipole components of the electronic potential were included up to $l = 14$. Furthermore, no contractions were applied in the continuum calculations to achieve maximum flexibility. Further details on the LDKL-DF method may be found elsewhere.[8,9]

(34) Ulbricht, P.; Häberlen, O. D.; Weinelt, W.; Steinrück, H. P.; Rösch, N. *Surf. Sci.* **1995**, *326*, 53.
(35) Ronova, I. A.; Alekseeva, N. V.; Veniaminov, N. N.; Kravers, M. A. *J. Struct. Chem. (Engl. Transl.)* **1975**, *16*, 441−443.
(36) Cox, A. P.; Brittain, A. H. *Trans. Faraday Soc.* **1970**, *66*, 557.
(37) Fan, L.; Ziegler, T. *J. Chem. Phys.* **1991**, *95*, 7401.
(38) Bodenheimer, J. S.; Low, W. *Spectrochim. Acta* **1973**, *29A*, 1733.
(39) Crichton, O.; Rest, A. J. *J. Chem. Soc., Dalton Trans.* **1977**, 986−993.
(40) Huber, K. P.; Herzberg, G. *Molecular Spectra and Molecular Structure Constants of Diatomic Molecules*; Van Nostrand: New York, 1979.

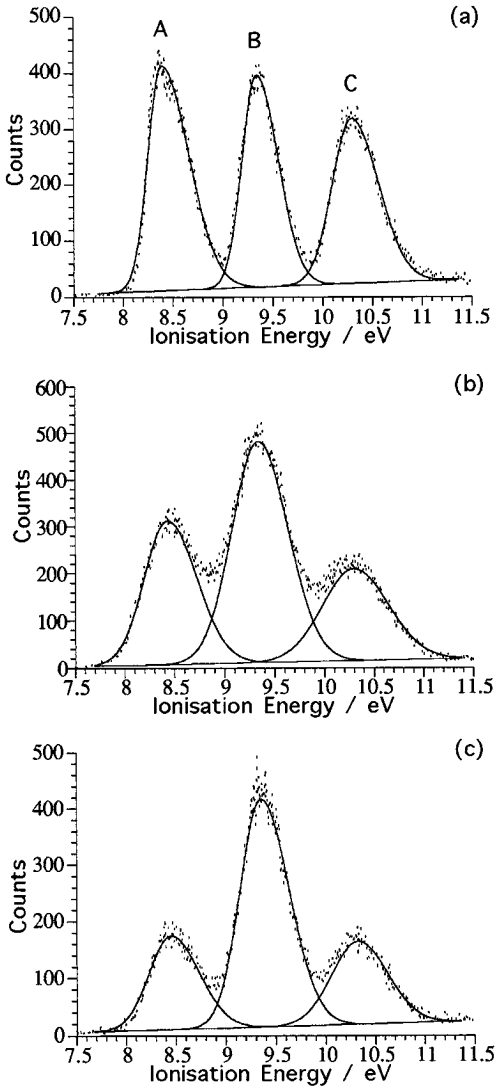

Figure 1. Photoelectron spectra of Ni(η^5-C_5H_5)(NO) obtained at incident photon energies of (a) 30, (b) 56, and (c) 70 eV.

Results and Discussion

Consideration of the Spectra. PE spectra of Ni(η^5-C_5H_5)(NO) in the ionization energy (IE) region 7.5−11.5 eV generated by synchrotron radiation at three different photon energies are shown in Figure 1. This region contains the three lowest IE bands of the compound, A−C. Relative partial photoionization cross sections (RPPICS) and branching ratios (BR) for bands A−C are shown in Figures 2 and 3, respectively. He I and He II spectra are shown in Figure 4.

It is immediately apparent that the central band B, which is the lowest in intensity at low photon energies, becomes the most intense above *ca.* 40 eV and comes to dominate this region of the spectrum at high photon energies. All three bands show an initial fall-off in cross section though this is steepest for band A.

These trends give an indication of the atomic character of the molecular orbitals from which the electrons are ionizing.[6] Theoretical atomic cross sections[41] for Ni 3d, C 2p, N 2p, and O 2p are shown in Figure 5. These plots provide a good guide to the qualitative variation of atomic photoionization cross sections. The Ni 3d orbital cross section is predicted to rise from threshold to a delayed maximum around 56 eV whereas the 2p cross sections of the light atoms fall. Overall, the cross section ordering within this series is O 2p > N 2p > C 2p.

The initial decay in the molecular cross sections of bands A−C is attributable to their ligand character, and the increase in intensity of the central band B shows it to have the most pronounced metal character. The break in the fall-off of cross section around 42 eV of bands A and C indicates that they also have some metal character. At high photon energies, the metal character dominates the cross section behavior. The fact that the branching ratio of band C is greater than that of band A may well indicate that C's metal character is higher, but different proportions of ligand contributions could also account for this level of variation.

Band B displays a pronounced minimum in its RPPICS at a photon energy of 68 eV. This feature in the RPPICS of band B between *ca.* 60 and 70 eV is attributable to the interference effect between the direct ionization of nickel 3d electrons and the resonant photoemission of 3d electrons in the region of a 3p → 3d giant resonant absorption. This feature lies in the photon energy region where excitation of the nickel atom 3p subshell, with binding energies of $3p_{3/2}$ = 73 eV, $3p_{1/2}$ = 75 eV in the free atom,[42] is likely to occur, leading to cross-sectional enhancement of 3d ionization processes. It may be compared with the 3p → 3d resonance photoabsorption and "super Coster−Kronig" decay observed in atomic nickel vapor at 64.3−68.5 eV.[43] Similar resonances have been found in PICS of other Ni compounds, notably in the RPPICS of the first two bands in Ni(η^5-C_5H_5)$_2$ which contain ionizations from orbitals of high nickel 3d character; here both bands show minima in their RPPICS at a photon energy of 65 eV.[44] In the RPPICS of Ni(PF_3)$_4$, a maximum is observed at 75 eV in the d ionization bands.[45] The shape of the feature found for Ni(η^5-C_5H_5)(NO), i.e. that of a gradual decrease in RPPICS as the photon energy is increased from 60 eV to a distinct minimum at about 68 eV followed by a sharp return to the overall behavior of the photoionization cross section, is a characteristic Fano profile found when the resonance process is relatively weak. A similar profile is found for the d band of ferrocene.[23] It may be taken as an indicator of significant Ni 3d character for the MO giving rise to band B. A similar but much weaker dip is just detectable in the profile of the RPPICS of band C.

Band A shows a high-energy shoulder which has previously been assigned to the $^2A_1$ ion state, the main part of band A being attributed to a $^2E_1$ ion state.[1] In order to search for cross-section variations between the various regions of this band, we obtained spectra with a 2.3 V pass energy between the photon energies of 18 and 32 eV. The upper limit was constrained by the fact that the lens was not able to retard electrons of higher kinetic energy generated by higher photon energies. Examples of these spectra are shown in Figure 6. No apparent variation in relative cross section is evident. Band A was fitted with three asymmetric Gaussians, A_1, A_2, and A_3. Renormalized branching ratios for A_1, A_2, and A_3 were calculated for these high-resolution spectra and for the He I and He II spectra and are shown in Figure 7. The apparent lower height of the shoulder in the He I spectrum is a consequence of the higher resolution of this spectrum. The $A_1/A_2/A_3$ branching ratios are constant over the whole region, whereas those of bands B and

(41) Yeh, J. J. *Atomic and Nuclear Data Tables*; Gordon Breach: Langhorne, PA, 1993.

(42) Briggs, D. *Handbook of X-Ray and Ultraviolet Photoelectron Spectroscopy*; Heyden: London, 1977.

(43) Schmidt, E.; Schröder, H.; Sonntag, B.; Voss, H.; Wetzel, H. E. *J. Phys. B* **1983**, *16*, 2961.

(44) Brennan, J.; Cooper, G. C.; Green, J. C.; Payne, M. P.; Redfern, C. M. *J. Electron Spectrosc. Relat. Phenom.* **1993**, *66*, 101.

(45) Brennan, J. G.; Green, J. C.; Redfern, C. M. *J. Chem. Soc., Dalton Trans.* **1990**, 1907.

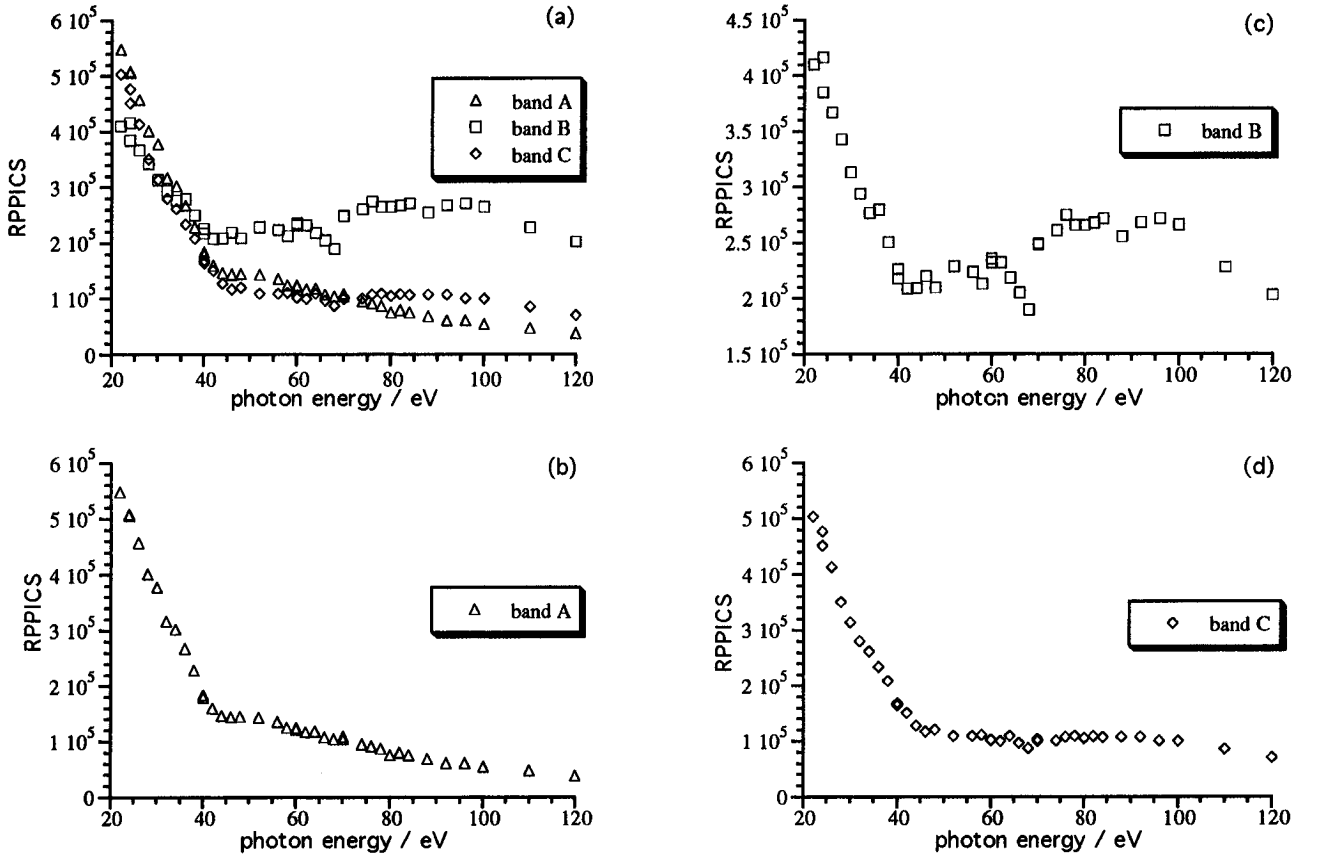

Figure 2. (a) RPPICS of bands A−C, (b) RPPICS of band A only, (c) RPPICS of band B only, and (d) RPPICS of band C only of Ni(η^5-C_5H_5)(NO).

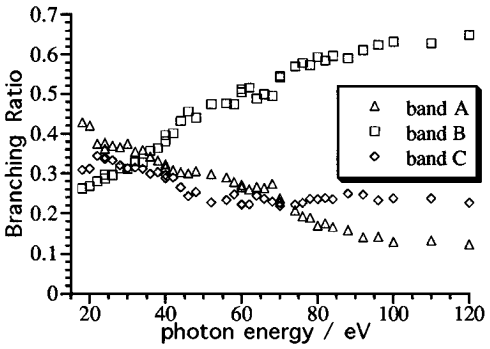

Figure 3. Branching ratios of bands A−C of Ni(η^5-C_5H_5)(NO).

C vary considerably. This is good evidence that the regions of band A represented by A_1, A_2, and A_3 have their origins in the same MO.

It can be seen from the He I spectrum (Figure 4b) that band B has a profile that, at high resolution, cannot be modeled with a single Gaussian, even an asymmetric one. It has a sharp center and two ill-defined shoulders, one on the low-energy and one on the high-energy side. This could be taken as evidence of more than one primary ionization process occurring in this region, but vibronic structure associated with just one ionization process cannot be ruled out.

Electronic Structure of Ni(η^5-C_5H_5)(NO). A simple picture of the electronic structure of the molecule Ni(η^5-C_5H_5)(NO) may be formed by building it from the fragments Ni(η^5-C_5H_5) and NO (see Figure 8).

The electronic structure of the first fragment is easily understood by considering the interaction of the C_5H_5 ring π orbitals and the valence orbitals of Ni. The cyclopentadienyl ligand and the metal both possess valence orbitals of e_1 symmetry, which are anticipated to be comparable in energy. Thus they interact strongly, forming a bonding as well as an antibonding pair of MOs of e_1 symmetry, but provide little net ring−metal bonding since they are almost completely filled, holding a total of seven electrons. The other occupied MOs are the Ni e_2 orbitals d($x^2 - y^2$, xy), which are primarily nonbonding, as back-donation to the cyclopentadienyl ring e_2(π^*) orbital is small, and the a_1 orbital, which is mainly of metal d(z^2) character, as its overlap with the ring a_1(π) orbital is small. This interaction analysis is supported by a LCGTO-DF calculation for Ni(η^5-C_5H_5) (see Figure 8), which also shows that the two sets of e_1 orbitals bracket the nonbonding metal orbitals e_2 and a_1.

For the second fragment, NO, only the $2\pi^*$ MO has to be taken into account as the other orbitals, 5σ, 1π, and 4σ, are too tightly bound to interact strongly (Figure 8). The set of $2\pi^*$ orbitals, also of e_1 symmetry, interact mainly with the higher lying e_1 set of the first fragment Ni(η^5-C_5H_5). Results of the LCGTO-DF calculations show that the metal−NO bonding partner of this interaction, $8e_1$, is mainly located on (η^5-C_5H_5)-Ni whereas the antibonding partner, $9e_1$, exhibits significantly more NO character. The other valence orbitals of Ni(η^5-C_5H_5) remain essentially unchanged (Table 1) and form the orbitals $7e_1$, $4e_2$, and $15a_1$. This interaction between the two fragments has two main consequences. The bonding between the C_5H_5 ring and the metal is strengthened as the ring−metal antibonding orbital $8e_1$ is now delocalized onto the second fragment. Furthermore, NO acquires an overall negative charge (−0.14 au) via this back-bonding. Nevertheless, the $2\pi^*$ MO participates only to a moderate extent in the HOMO $8e_1$ of Ni(η^5-C_5H_5)(NO) whereas the LUMO $9e_1$ features a strong localization on NO (Table 1). The Mulliken charge of the C_5H_5 ring is −0.25 au, and the corresponding configuration of the Ni atom is $s^{0.52}p^{0.43}d^{8.66}$ (charge: +0.39 au). The metal character,

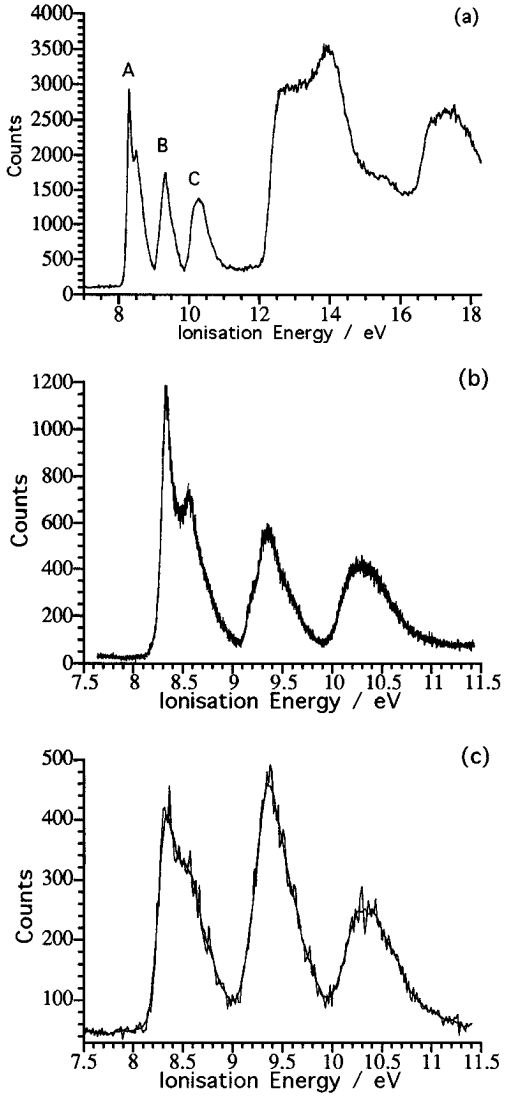

Figure 4. (a) He I 7−18.3 eV, (b) He I 7.5−11.5 eV, and (c) He II 7.5−11.5 eV photoelectron spectra of Ni(η^5-C_5H_5)(NO).

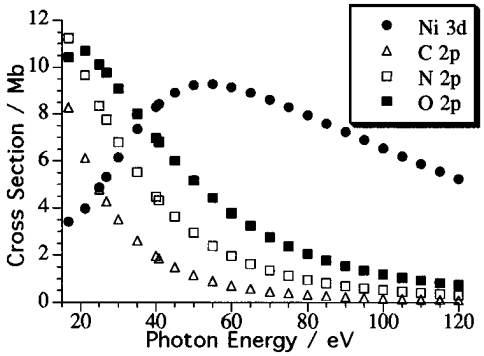

Figure 5. Calculated atomic cross sections for Ni 3d, C 2p, N 2p, and O 2p.

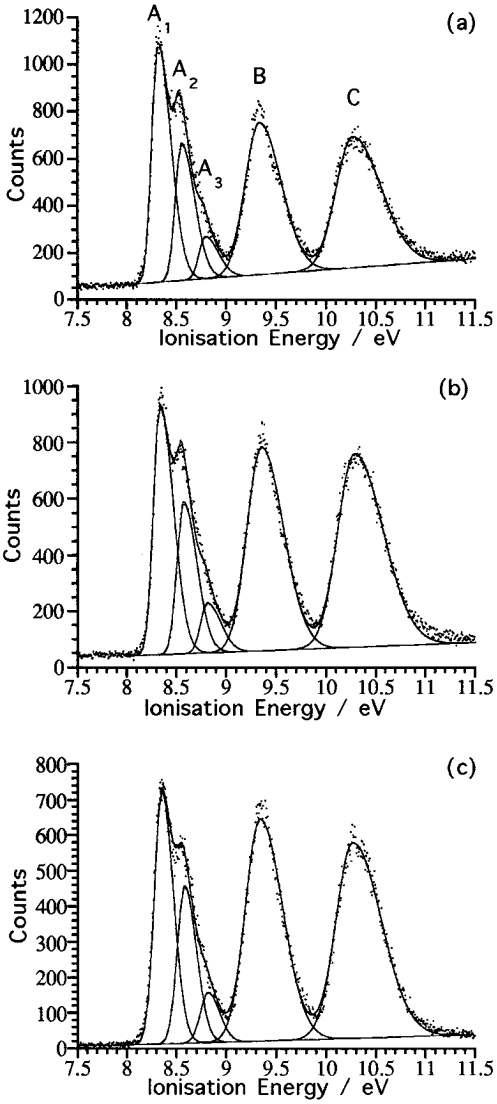

Figure 6. Photoelectron spectra of Ni(η^5-C_5H_5)(NO) collected at (a) 18 eV, (b) 22 eV, and (c) 28 eV using 2.3 V pass energy.

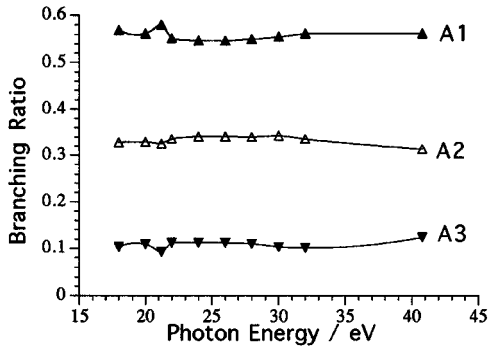

Figure 7. Branching ratios of bands A_1, A_2, and A_3 from high-resolution spectra over the photon energy range 18−40.8 eV.

especially the Ni 3d contribution, of the four highest lying occupied orbitals is of particular importance for the assignment of the PE spectra. Inspection of Table 1 reveals that the metal character is very high for the MOs $4e_2$ (96% d) and $15a_1$ (12% s, 77% d) and moderate for MO $7e_1$ (50% d), but rather low for the HOMO $8e_1$ (7% p, 15% d).

Contour plots of the the three highest occupied orbitals of the a_1 and the e_1 manifolds as calculated by the LCGTO-DF method illustrate the interaction analysis just presented (Figures 9 and 10). Particular attention is drawn to the fact that the MO $7e_1$ is ligand-to-metal bonding, in particular to the C_5H_5 ring ligand, whereas MO $8e_1$ contributes mainly to the metal−nitrosyl bonding via back-donation into the $2\pi^*$ orbital of NO, but is antibonding with respect to the cyclopentadienyl ring. This analyis agrees very well with the calculated results for the changes of the geometry and of the vibrational frequencies upon going from the neutral molecule to the cation (Table 2). The calculated changes in the NO-related quantities fully support the present MO analysis. Ionization of MO $8e_1$ reduces the back-donation from the metal to the nitrosyl ligand, thus elongating the metal−ligand bond and shortening the N−O bond. Concomitant frequency changes are calculated for the

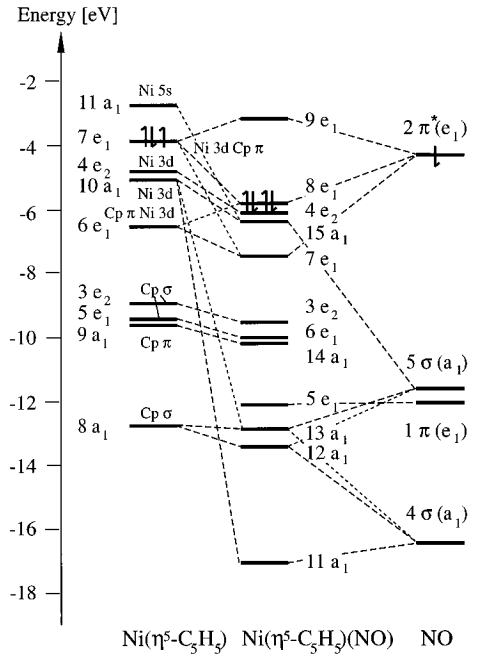

Figure 8. Orbital interaction diagram of the fragments Ni(η^5-C_5H_5) and NO forming Ni(η^5-C_5H_5)(NO) based on the Kohn−Sham one-electron energies (spin-averaged for the fragments) of LCGTO-DF calculations. For the highest occupied level of each system, the occupation is indicated.

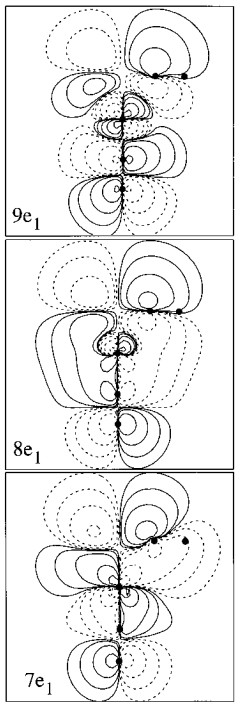

Figure 9. Contour plots of the molecular orbitals $7e_1$, $8e_1$ (HOMO), and $9e_1$ (LUMO) of Ni(η^5-C_5H_5)(NO) in a plane containing the axis O−N−Ni as well as one C and one H atom (see **1**). The contour lines correspond to values of the wave function of 10^{-n} au, $n = 1.0$, 1.5, 2.0, and 2.5; solid and dashed lines represent values of opposite signs. The locations of the nuclei are marked by dots.

two corresponding vibrational modes affected by the NO ligand (e.g. about +70 cm^{-1} for ν(N−O)). Of course, there is still significant back-bonding in the cation ground state, $^2E_1$, as can be seen by comparing the N−O vibrational frequency for Ni(η^5-C_5H_5)$(NO)^+$, 1911 cm^{-1}, and that for the free ion NO^+, 2344 cm^{-1} (Table 2). On the other hand, the orbitals of the a_1 manifold contribute to this bonding only to a lesser degree. A sizable Ni 4s admixture to the metal-based MO $15a_1$ can be

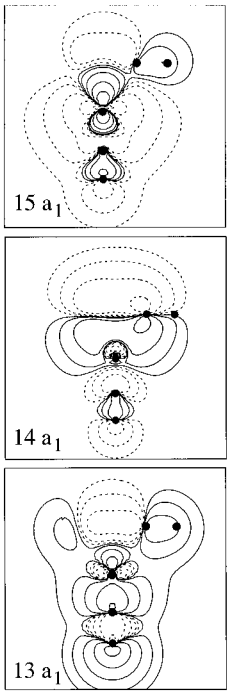

Figure 10. Contour plots of the molecular orbitals $13a_1$, $14a_1$, and $15ae_1$ of Ni(η^5-C_5H_5)(NO). Layout is as in Figure 9.

seen. MO $14a_1$ has mainly C_5H_5 π character (88%), and the NO 5σ contribution makes up most of MO $14a_1$ (72%).

Ionization Energy Calculations for Ni(η^5-C_5H_5)(NO). Photoionization energies were calculated using Slater's transition state method[46] and the ΔSCF approach (taking total energy differences between the ionic and the ground state). Both the LDA and the GGA exchange-correlation functional were employed (see Table 3) at the GGA-optimized geometry, except where noted. Besides the ionization energies of the four highest lying states that are crucial for the assignment of the experimental PE spectrum, the next three larger ionization energies are displayed in Table 3. The corresponding transitions involve MOs of the C_5H_5 ring, namely the remaining π orbital, $14a_1$, as well as the two highest lying s MOs $3e_2$ and $6e_1$. In general, the transition state approximation turns out to be quite accurate, deviation from ΔSCF values are about 0.2 eV at most. To explore the sensitivity of the computational procedure, LDA transition state ionization potentials were also calculated for the experimental geometry, resulting in values that are in most cases about 0.3 eV higher. Note however, that the ordering and the relative spacings of the ionization energies remain unaffected by all variations explored in the present investigation: different exchange-correlation functionals, alternative computational strategies to access the ionization energy (transition state vs ΔSCF), or a moderate change of the geometry.

Thus, all these computational variants yield rather similar ionization energies; in particular, the level ordering is identical in all cases (Table 3). The lowest five ionization energies calculated with the ΔSCF procedure at the GGA level of theory agree exceptionally well with experiment and confirm the assignment to be described below in detail. As often with a density functional based method, the higher lying ionization energies, starting with those corresponding to the levels $14a_1$ and $6e_1$, are calculated somewhat too low in energy.

The level splitting pattern of the first four ionization energies, especially the gap of about 1 eV between the first two ionization

(46) Slater, J. C. *The Self-Consistent Field for Molecules and Solids: Quantum Theory of Molecules and Solids*; McGraw-Hill: New York, 1974; Vol. 4.

Table 3. Ionization Potentials of Ni(η^5-C_5H_5)(NO) Obtained by LCGTO-DF Calculations at Both LDA and GGA Levels of Theory for the GGA-Optimized Geometry (Except for One Case) Compared to Results from Other Computational Methods (MS−Xα, INDO) and to Experiment[a]

	LCGTO-DF/LDA[b]			LCGTO-DF/GGA[b]					MS−Xα		
orbital	TS	TS[d]	ΔSCF[f]	GS[d]	TS	Δ(TS−GS)	ΔSCF	expt[b]	GS[e]	TS[f]	INDO[c]
$8e_1$	8.35	8.61	8.49	5.79	8.53	2.74	8.31	8.33/8.56	4.97	7.7	7.83
$15a_1$	9.46	9.76	9.64	6.37	9.71	3.34	9.36	9.35	5.92	8.6	8.89
$4e_2$	9.77	10.06	10.01	6.16	9.95	3.79	9.83	9.35	6.85	9.7	9.26
$7e_1$	10.52	10.80	10.60	7.75	10.69	2.94	10.38	10.28	7.43	10.0	9.93
$3e_2$	12.46	12.42	12.48	9.59	12.49	2.90	12.45	12.64	11.13		
$14a_1$	12.91	13.22	12.98	10.21	13.11	2.90	12.91	13.90	9.17		
$6e_1$	12.99	12.89	12.98	10.19	12.99	2.80	12.98	13.90	11.86		

[a] Ionization energies are calculated both by the Slater's transition state method (TS) and by taking total energy differences of the ionic and the ground states (ΔSCF). Also shown are the (negative of the) Kohn−Sham ground state eigenvalues (GS) as well as their relaxation energies Δ(TS−KS) upon going from the ground state to the transition state. All energies are in electronvolts. [b] Present work. [c] Reference 3. [d] Experimental geometry of reference 35. [e] Reference 15. [f] Reference 5.

energies, is also well reproduced by other computational approaches, like the INDO method[3] and the MS−Xα method.[5] The energy difference of the next two ionization energies, $15a_1$ and $4e_2$, is of importance for the assignment of band B in the experimental PE spectra. Clearly, the similarly strong metal character of these two orbitals suggests a small energy difference, but this is calculated only by the LCGTO-DF method (0.47 eV) and by the INDO method (0.33 eV) whereas the MS−Xα results[5,15] (see Table 1) make an assignment to one, even a broad, band less probable.

A noteworthy feature of the present calculations is the different ordering of levels $15a_1$ and $4e_2$ in the ground state and the transition state calculations. In the framework of Hartree−Fock theory, such a rearrangement is often referred to a breakdown of Koopmans' theorem,[47] which refers to the fact that the straightforward interpretation of an orbital energy as the (negative of the) corresponding ionization potential no longer holds and one has to refer to a ΔSCF procedure. In this way, the relaxation of the ionic state is taken into account, thus leading to a lower value of the ionization energy. On the other hand, Koopmans' theorem does not hold in density functional theory[46] and the Kohn−Sham one-electron energies lack a direct physical interpretation. However, Slater's transition state concept[46,48] links an ionization energy to the (negative of the) orbital energy of a configuration "halfway" between the initial and the final state of an ionization process. The resulting orbital energy relaxation, i.e. the difference of the one-electron energy in the ground and the transition state, is related to the Coulomb self-interaction of the electron being removed.[46,49] Therefore this type of relaxation always increases the value of the orbital energy in the transition state, the amount depending on the localization of the orbital under consideration. It is in general larger for a localized transition metal d orbital than for a ligand-derived, extended orbital and may thus lead to a reordering of the one-electron-level spectrum in the transition state. Ni(η^5-C_5H_5)(NO) provides a rare example. The transition state relaxation Δ(TS−KS) of the lowest ionization potentials is about 2.8−2.9 eV with the exception of the highly localized orbitals $15a_1$ and $4e_2$ (see Table 3) where 3.34 and 3.79 eV are calculated at the GGA level of theory. There is an obvious correlation of the size of this relaxation and the Ni d character of the various orbitals, 77% and 96% (see Table 1).

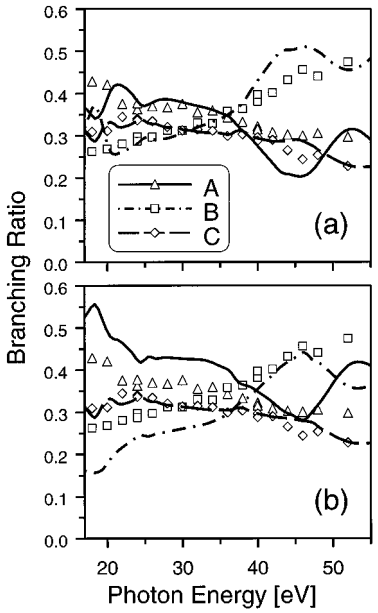

Figure 11. Branching ratios for the first three bands of the photoelectron spectrum of Ni(η^5-C_5H_5)(NO) as obtained by LDKL-DF calculations compared to experiment: (a) present assignment with band A comprising ionization from MO $8e_1$, B from MOs $15a_1$ + $4e_2$, and C from MO $7e_1$; (b) previous assigment of refs 1, 2, and 15 with band A comprising ionization from MOs $8e_1$ + $15a_1$, B from MO $4e_2$, and C from MO $7e_1$. Calculated results for bands A−C are shown as lines (solid, dot-dashed, and dashed, respectively); measured results, as symbols (triangles, squares, and diamonds, respectively).

Photoionization Cross Section and Branching Ratio Calculations. To support the new assignment of the PE spectra, it seemed useful to calculate photoionization cross sections for Ni(η^5-C_5H_5)(NO) and to compare calculated to measured branching ratios for the various PE spectra comprising bands A, B, and C. This allows also a check of the two competing assignments of bands A and B, the present one and that of refs 1, 2, and 15. Only the results for the branching ratios will be shown (see Figure 11) and discussed in the following. The cross-section calculations had to be restricted to photon energies below 55 eV in order to keep the computational effort manageable. For higher values of the asymptotic kinetic energy of the photoelectron, still more flexible continuum basis sets would be required in the LDKL-DF calculations. Yet in the energy range investigated, the decisive onset in the rise of the branching ratio for band B which is due to the high Ni d contribution is already clearly visible.

The agreement of calculated and experimental branching ratios is very good for photon energies up to about 40 eV if based on the present assignment. The competing assign-

(47) Veillard, A.; Demuynk, D. In *Methods of Modern Theoretical Chemistry, Vol. 4;* Schaefer, H. F., Ed.; Wiley: New York, 1977; p 171.
(48) Janak, J. F. *Phys. Rev. B* **1978**, *18*, 7165.
(49) Rösch, N. In *Electrons in Finite and Infinite Systems;* Phariseau, P., Scheire, L., Eds.; NATO Advanced Study Institute, Series B, Vol. 24; Plenum Press: New York, 1977; p 1.

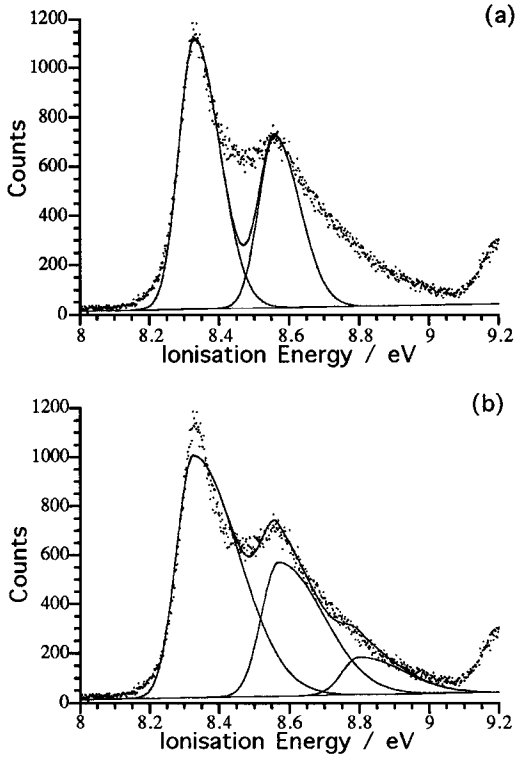

Figure 12. He I spectra of band A of (η^5-C_5H_5)Ni(NO) fitted using (a) two Gaussians of equal asymmetric widths and (b) three equally spaced Gaussians of equal asymmetric widths.

ment,[1,2,15] with $^2E_1$ and $^2A_1$ ion states collected in band A and just state $^2E_2$ in band B, does not yield convincing branching ratios (see Figure 11b). Of course, the branching ratio for band C is not in dispute, but the perfect agreement of calculated and experimental results lends additional credibility to the computational method employed and to the assignment proposed here. The rise of the branching ratio of band B above 40 eV photon energy due to the high metal character is clearly reflected by the LDKL-DF results. As a matter of fact, the photoionization cross section for the $^2A_1$ ion final state is calculated somewhat too large for these energies, leading to an overestimation of the branching ratio for band B in our assignment and apparently better agreement between 40 and 48 eV for the alternative assignment. This is a consequence of the fact that the present continuum basis set results in a decrease of quality for the LDKL-DF results for photon energies above 40 eV. Despite these limitations of the present LDKL-DF calculations, they are able to reproduce the experimental branching ratios much better than an investigation using the continuum MS−Xα method.[15]

It is at high photon energies where the assumption that photoelectron cross sections are largely determined by the nature of the atomic cross section of the contributing atomic orbitals holds best. Also, as discussed above, the Ni 3d cross section in the region of 100 eV is estimated to be about 6 times larger than the ligand 2p cross sections. We can, therefore, make an estimate of the branching ratios at this energy solely on the basis of the calculated Ni 3d content of the MO and compare the two competing assignments. The predicted branching ratios are as follows: $8e_1$, 0.08; $15a_1$, 0.19; $4e_2$, 0.48; $7e_1$, 0.25. Our assignment therefore predicts A/B/C branching ratios of 0.08/0.67/0.25 wheres the original assignment would give 0.27/0.48/0.25. The former is in considerably better agreement with the experimental values at 100−110 eV of 0.13/0.63/0.24. Any inclusion of the ligand contribution will *increase* the prediction for band A and *decrease* the prediction for band B, thus

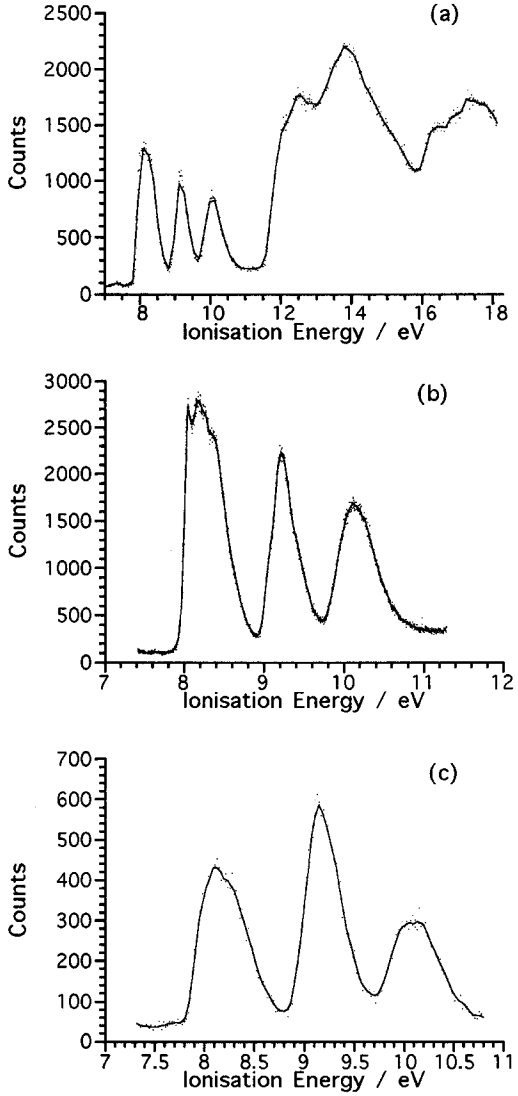

Figure 13. (a) He I 7−18.3 eV, (b) He I 7.5−11.5 eV, and (c) He II 7.5−11.5 eV photoelectron spectra of Ni(η^5-$C_5H_4CH_3$)(NO).

improving agreement with our assignment while *worsening* agreement with the original assignment.

Reconciliation of Experimental and Theoretical Results. The photoionization cross-section and the MO calculations provide a consistent picture of the electronic structure and indicate that the correct assignment of the photoelectron bands is the one which associates band A just with the $^2E_1$ ground state of the molecular ion, band B with *both* the $^2E_2$ and $^2A_1$ ion states, and band C with the $^2E_1$ excited state. Both the calculated IEs and the calculated metal composition of the orbitals concur closely with the experimental observations with this interpretation.

Such an assignment leaves two questions unanswered: first, the cause of the high-energy shoulder of band A and, second, the assignment of the PE spectrum of Ni(η^5-$C_5H_4CH_3$)(NO), where the published spectrum shows a shoulder on the low-energy band of band A.

Origin of the Structure on Band A. The first band of He I PE spectrum of Ni(η^5-C_5H_5)(NO) is shown in Figure 12 fitted with two equal-width and three equal-width asymmetric Gaussians. Two asymmetric Gaussians are clearly inadequate for fitting the higher resolution He I spectrum. Three asymmetric Gaussians give a much improved fit, but it is apparent that there is additional structure in the band. Notably the sharpness of the first maximum is not well modeled, which suggests another

Table 4. IE (eV), Ion States, and Corresponding Molecular Orbitals for the PE Spectra of Ni(η^5-C_5H_5)(NO) and Ni(η^5-$CH_3C_5H_4$)(NO)

band	ionization energies		ion states	MOs
	Ni(η^5-C_5H_5)(NO)	Ni(η^5-$C_5H_4CH_3$)(NO)		
A	8.33, 8.56	8.05, 8.17, 8.35 sh	$^2E_1$	$8e_1$
B	9.35 (9.22 sh, 9.52 sh)	9.22 (9.09 sh, 9.41 sh)	$^2A_1$, $^2E_2$	$15a_1$, $4e_2$
C	10.28	10.12	$^2E_1$	$7e_1$
	12.64	12.50	$^2E_2$	$3e_2$ (C−C σ)
	13.90	13.82	$^2A_1$, $^2E_1$	$6e_1$, $14a_1$ (C−C σ)

progression to be probably present. However, the data seem not to justify the introduction of further Gaussians, as their number and shape would be somewhat arbitrary. The energy difference between the two maxima, as observed in the high-resolution He I spectrum, in band A is 0.23 (±0.01) eV, equivalent to 1855 (±81) cm^{-1}. The energy separations of the three Gaussians used to produce the fit shown in Figure 8 are 0.24 and 0.23 eV. These estimates are very close to energy of the N−O stretching mode observed in the infrared spectrum of Ni(η^5-C_5H_5)(NO) at 1832 cm^{-1}.[39] For comparison, the vibrational energy of the first ionization band of NO is 2260 cm^{-1},[50] which corresponds to ionization of the single unpaired electron in the $2\pi^*$ orbital; this is significantly higher than the N−O stretching mode at 1876 cm^{-1} seen in the infrared spectrum of nitric oxide.[40] We, therefore, assign the shoulder to an excitation of an N−O stretch.

The 29% NO character calculated for the $8e_1$ orbital would account for such a vibrational excitation. As the predicted NO contribution to the $8e_1$ level is NO antibonding in character, the contributing MO being $2\pi^*$, ionization of the $8e_1$ level to the cation strengthens the N−O π bond, and thus the NO stretching frequency is slightly larger than for the neutral species, as found in the corresponding calculations for the cation (Table 2). In Ni(η^5-C_5H_5)$(NO)^+$, the N−O bond length is calculated to decrease by about 0.03 Å compared to that of the neutral molecule, so ionization to the $^2E_1$ ground state is likely be accompanied by Franck−Condon-induced vibrational excitations. The calculated value of 1911 cm^{-1} for the NO stretching mode in [Ni(η^5-C_5H_5)$(NO)]^+$ falls within the range 1855 ± 81 cm^{-1} given by experiment.

Cyclopentadienyl e_1 ionizations commonly show structure. For example, the e_{1g} ionization of Mg(η^5-C_5H_5)$_2$ shows a progression due to excitation of the e_{1g} ring stretching mode as a result of dynamic Jahn−Teller distortion of the $^2E_{1g}$ ion state.[51] Similar Jahn−Teller behavior here could be the reason for additional vibrational structure in the PE band, as the calculation shows orbital $8e_1$ to have significant cyclopentadienyl character.

PE Spectrum of Ni(η^5-$C_5H_4CH_3$)(NO). The published PE spectrum of Ni(η^5-$C_5H_4CH_3$)(NO) shows a shoulder on the low-energy side of band A apparently analogous to the high-energy shoulder in the PE spectrum of Ni(η^5-C_5H_5)(NO). We remeasured the spectrum of Ni(η^5-$C_5H_4CH_3$)(NO) using both He I and He II radiation; the spectra are shown in Figure 13, and IE data are given in Table 4. Branching ratios for bands A−C are given in Table 5. The branching ratios for the three main bands are very similar to those of Ni(η^5-C_5H_5)(NO).

There is a difference in the structure of the first band A from that shown in the published spectrum. In our spectrum there are three discernible maxima at 8.05, 8.17, and 8.35 eV. The published spectrum shows two at 8.09 and 8.32 eV. There could be several reasons for the discrepancy such as lower resolution, a small impurity distorting the peak profile, or a pressure variation during the original slow scan in the earlier work. The main conclusion is that the proposed shift in the a_1 ionization from 8.48 to 8.09 eV[1] can be discounted.

Table 5. Relative Intensities (Branching Ratios) for Bands A−C in the He I and He II Spectra of Ni(η^5-$C_5H_4CH_3$)(NO)

band	He I	He II
A	0.44	0.36
B	0.27	0.40
C	0.29	0.24

The fine structure observable on band A in the PE spectrum of Ni(η^5-$C_5H_4CH_3$)(NO) differs from that of the unmethylated compound. Methylation of the ring lifts the degeneracy of the e_1 orbitals of cyclopentadienyl; thus the associated ionizations no longer achieve a degenerate ion state. This is expected to lead to a more complex band structure, as is indeed found.

The intensity variations in the first three bands of the PE spectrum of Ni(η^5-$C_5H_4CH_3$)(NO) are given in Table 5. A pattern very similar to that discussed above is found. The IE shifts on methylation are also consistent with the new band assignment but were problematic with the old one. Typical shifts on dimethylating metallocenes are 0.19 eV for metal bands, 0.24 eV for e_{1g} bands, and 0.26 eV for e_{1u} bands, all to lower IE.[52] Band A shifts most by 0.28 eV, band B shifts least by 0.13 eV, and band C shows intermediate behavior, shifting by 0.16 eV. This is consistent with the relative amounts of cyclopentadienyl character calculated for the associated orbitals.

Other Work. During the course of this work we learned that branching ratio data on the low-IE PE bands Ni(η^5-C_5H_5)(NO) had also been obtained by Bancroft *et al.*, who report their findings in a paper parallel to this.[15] The experimental findings are in good agreement with our own but they favor the original assignment of ionization of both the $8e_1$ and the $15a_1$ orbitals as giving rise to band A. This is in part due to their IE and branching ratio calculations (using the contiuum MS−Xα method) being in better agreement with the original assignment and in part a result of a different deconvolution of band A. We have considered their evidence but find that the weight of the arguments presented above is in favor of our new assignment.

Conclusions

The PE spectrum shows three low-energy bands, A−C, assigned to the ion states (MO): $^2E_1$ ($8e_1$) (A) < $^2A_1$ ($15a_1$) + $^2E_2$ ($4e_2$) (B) < $^2E_1$ ($7e_1$) (C). We reach this conclusion on the basis of the following evidence.

Consideration of the qualitative trends in ionization cross sections of these three PE bands of Ni(η^5-C_5H_5)(NO) suggests that band B arises from MOs of preponderant metal character, that band C is associated with orbitals of some metal character, and that band A comes from orbitals of largely ligand character. No cross-sectional variation is found within the regions of band A, indicating that it is associated with a single ion state.

Density functional calculations indicate an orbital character consistent with these qualitative trends. Ionization energies

(50) Turner, D. W.; Baker, C.; Baker, A. D.; Brundle, C. R. *Molecular Photoelectron Spectroscopy*; Wiley-Interscience: London, 1970.
(51) Bähr, A.; Cooper, G.; Green, J. C.; Longley, K. A.; Lovell-Smith, M.; McGrady, S. *Chem. Phys.*, submitted.
(52) Green, J. C. *Struct. and Bonding* **1981**, *43*, 37−112.

calculated by a variety of methods are in excellent agreement with this assignment but are difficult to reconcile with the alternative assignment of both a $^2E_1$ and a $^2A_1$ ion state to band A. Branching ratio calculations also show overall trends which agree well with the experimental data, together with the new assignment.

The separation of the principal fine structure that we can identify in band A is consistent with an excitation of the N−O stretch.

The MO model proposed on the basis of the DF calculations is justified by the good agreement it gives with the ground state structure and the vibrational frequencies as well as the ionization energies and cross-section data. Population analysis assigns a small positive charge to the Ni center and negative charges to both ligands. The large majority of metal−ligand bonding occurs through the $7e_1$ and $8e_1$ orbitals and can be visualized as π donation from the cyclopentadienyl ligand (formally taken as anion) and π back-donation to the NO ligand. This picture is in contrast with the oxidation state formalism of linear η^1-NO as NO^+.

The combination of variable-photon-energy photoelectron spectroscopy and high-level density functional calculations of both ionization energies and branching ratios has led to a new assignment of the PE spectrum of Ni(η^5-C_5H_5)(NO) and a firmly based model of the electron distribution in this key molecule.

Acknowledgment. This work was supported by the Deutsche Forschungsgemeinschaft, the Volkswagen-Stiftung, the Fonds der Chemischen Industrie, and the SERC.

IC951120O